Hindawi

Research Article

Time-Dependent Fuzzy Reliability Analysis of Concrete Slab during the Initial Water Storage Period of CFRD: A Case Study

Gang Sun [iD],[1] **Kongzhong Hu** [iD],[2,3] **Lifang Liu** [iD],[4] **and Junru Li** [iD][3,4]

[1]*College of Urban and Rural Construction, Zhongkai University of Agriculture and Engineering, No. 501, Zhongkai Road, Guangzhou, China*
[2]*College of Chemistry and Civil Engineering, Shaoguan University, No. 288, Daxue Road, Shaoguan, China*
[3]*College of Water Resource and Hydropower, Sichuan University, No. 24 South Section 1, Yihuan Road, Chengdu, China*
[4]*School of Civil and Environmental Engineering, Harbin Institute of Technology (Shenzhen), Shenzhen, China*

Correspondence should be addressed to Junru Li; lijunru@hit.edu.cn

The concrete-faced rockfill dam (CFRD) has been widely constructed worldwide, and the reliability of the concrete panels, the most important containment structure, is critical to the safety of the CFRDs and downstream communities. Several practical projects show that concrete slab cracking usually occurs during the water storage period, which can be attributed to the rapid increase of hydrostatic pressure and uneven settlement of the dam body. In this paper, a time-dependent reliability analysis method considering the fuzziness of the failure criterion is presented to assess the slab cracking risk of the Houziyan CFRD during the water storage period. Based on the observed deformation, the material parameters are calibrated to ensure the fidelity of the numerical simulation. Based on the Drucker–Prager yield criterion and tensile strength criterion, the response surface method is utilized to construct the performance functions at different moments, and then the time-dependent reliability analysis considering the fuzzy failure criteria is implemented for the concrete slab. The case study of the Houziyan CFRD shows that, during the initial period of water storage, the reliability index of the concrete slab decreases with the rise of the water level. With a stable water level, the probability of cracking of the concrete slab slowly decreases as the deformation of the dam body and slab tend to be coordinated. Especially, considering the fuzziness of the failure criteria, the reliability index decreased by about 2%, indicating that the proposed evaluation method is biased toward safety. The method proposed in this paper can reflect the evolution law of concrete slab reliability with the operating environment and provides a new approach to evaluate the performance of the concrete slab during the water storage period.

1. Introduction

For the development of hydropower resources, many dams have been built, among which the concrete-faced rockfill dam (CFRD) is one of the most important types; the CFRD is a local material dam with low cost and good adaptability to the terrain [1, 2]. China has built a large number of CFRDs, such as Shuibuya, Houziyan, and Tianshengqiao-I. With the continued construction and operation of large numbers of CFRDs, the issue of ensuring the safety of these dams has gained widespread concern. One of the most important concerns of dam safety is the reliability of the concrete slab [3].

Different from concrete dams and core rockfill dams, the concrete slab is the most important impermeable structure of CFRDs. The lower structural strength and higher stress levels cause concrete slabs to be highly susceptible to cracking, which is a critical challenge for the safety of CFRDs. The damage to the concrete slab will directly lead to a decrease in seepage control performance and seepage damage or even dam breakage [4, 5], resulting in a series of associated geo-hazards, such as floods and landslides, which will cause devastating disasters to downstream buildings and residents [4–10].

The evaluation of the performance of the concrete slab is important for the operation control of CFRDs. The reliability

analysis, different from the factor of safety, demonstrates superiority by providing complete information regarding the risk levels revealed by a specific structure and has been widely applied to evaluate the safety performance of structures [3, 11], such as slope [12], tunnel [13], and bridge [14]. Research on the reliability analysis of CFRDs mainly focuses on the dam slope stability [15, 16], the concrete slab cracking [3, 17, 18], and the seismic response [19, 20]. For example, Kartal et al. [3, 17] considered the effects of hydrostatic and seismic loads on the safety performance of concrete slabs and obtained the reliability index of the concrete slab in the above cases using the FERUM reliability analysis program. Lu et al. [21] combined the idea of equivalent extreme events with the direct probability integral method and evaluated the seismic reliability of the CFRD based on the vertical deformation of the dam crest and the cumulative slippage of the dam slope. Liu et al. [22] established the limited state function of slab cracking based on the tensile stress criterion and analyzed the slab cracking probability of a CFRD in the operation period. Yang et al. [23] proposed a dynamic evaluation method of reliability in CFRDs and applied it to assess the risk of cracking in concrete slabs. The above research mainly focuses on the structural reliability of CFRD under a specific operating environment or operation period. The results show that the reliability of the slab varies with the operational loads and the mechanical response (e.g., deformation and stress) of CFRDs, i.e., the reliability of the concrete slab is time-dependent. However, changes in the operating environment and behavior of CFRDs are most dramatic during the initial water storage period, and slab cracking events also tend to occur during this stage [24, 25], which can be attributed to the increased hydraulic load and the incompatibility of the deformation between the concrete slab and the rockfill area. Therefore, it is more significant to study the slab safety performance of CFRD during the initial water storage period.

In addition, in the traditional reliability analysis, a performance function less than 0 indicates a panel cracking event, but in actual engineering, there is no strict threshold for determining whether the concrete structure is cracked or not [26], i.e., there is objective fuzziness in the damage criterion of the concrete slab. In our previous study [27], a method to estimate the time-dependent reliability of the slab using the health monitoring data was proposed, but without considering the fuzziness of the failure criterion, which has important implications for the safety of concrete slabs. The actual conditions of the normal use and durability of practical engineering structures should consider the fuzzy failure criterion, and so far, some fuzzy reliability analysis methods have been proposed. Ji [28] added a fuzzy stochastic variable to the performance function to reflect the fuzzy feature of the failure criterion and analyzed the fuzzy reliability by the stochastic response surface method (RSM). Chen et al. [29] improved the Latin hypercube sampling function to analyze the fuzzy damage probability of LDL dams for the case where the fuzzy failure criterion cannot be described. Ren et al. [30] introduced different membership functions to describe the fuzzy failure criteria, and the results show that the potential seismic vulnerability of bridges may be understated in the

absence of consideration of structural fuzzy failure criteria. Therefore, in the time-dependent reliability analysis of the concrete slab, the consideration of the fuzzy feature of failure criteria is necessary.

Given the above issues, this paper proposes a time-dependent fuzzy reliability analysis method to assess the failure probability and safety state of concrete slabs in CFRDs. The proposed methods consist of two main components, the first of which is similar to our previous study [27], i.e., the mechanical parameters are calibrated using deformation back analysis techniques, and the time-dependent performance function of slab cracking is constructed by the Drucker–Prager (DP) yield criterion and tensile strength criterion. The second component is novel; the membership function is introduced to describe the fuzziness of the failure criterion of concrete slabs, and the Monte-Carlo simulation (MCS) method for time-dependent fuzzy reliability analysis is proposed. It should be declared that, to compare with the reliability analysis without considering the fuzziness, in the case study, the same CFRD named Houziyan as in the study of Li et al. [27] is chosen. The main contributions can be summarized as follows:

(1) Based on a comprehensive literature review, to the best of our knowledge, this paper is the first to consider the fuzziness of the failure criterion in the reliability analysis of CFRDs.

(2) The mean values of the stochastic parameters are determined from an inverse analysis based on the observed deformations rather than assumptions, which is more reasonable for studying the safety of the concrete slab during the operation of an actual CFRD.

(3) The fuzzy failure probabilities of the concrete slab at different moments during the water storage period are investigated, which can provide a basis for the operational scheduling of CFRDs.

The rest of the paper is organized as follows: Section 2 presents an engineering overview and numerical model of the study area, i.e., the Houziyan CFRD. Section 3 describes the proposed method and provides the implementation process. The results are shown in Section 4, and the time-dependent fuzzy reliability of the concrete slab is also discussed. In Section 5, some conclusions are drawn.

2. Study Area

2.1. Project Overview. The studied CFRD named Houziyan is located in western China, and the typical section of the dam, which has a height of 223.5 m, is shown in Figure 1. From upstream to downstream, the dam can be roughly divided into the concrete slab, cushion layer, transition layer, upstream rockfill area, and downstream rockfill area, and the construction process of the dam body can also be found in Figure 1. Due to the high height of the dam, the concrete slab was not poured and formed at once, but in three phases, the elevation of slab construction seams are 1,695 and 1,797 m, respectively.

The Houziyan Hydropower Station is located in Southwest China's typical mountainous region [31]. The dam site
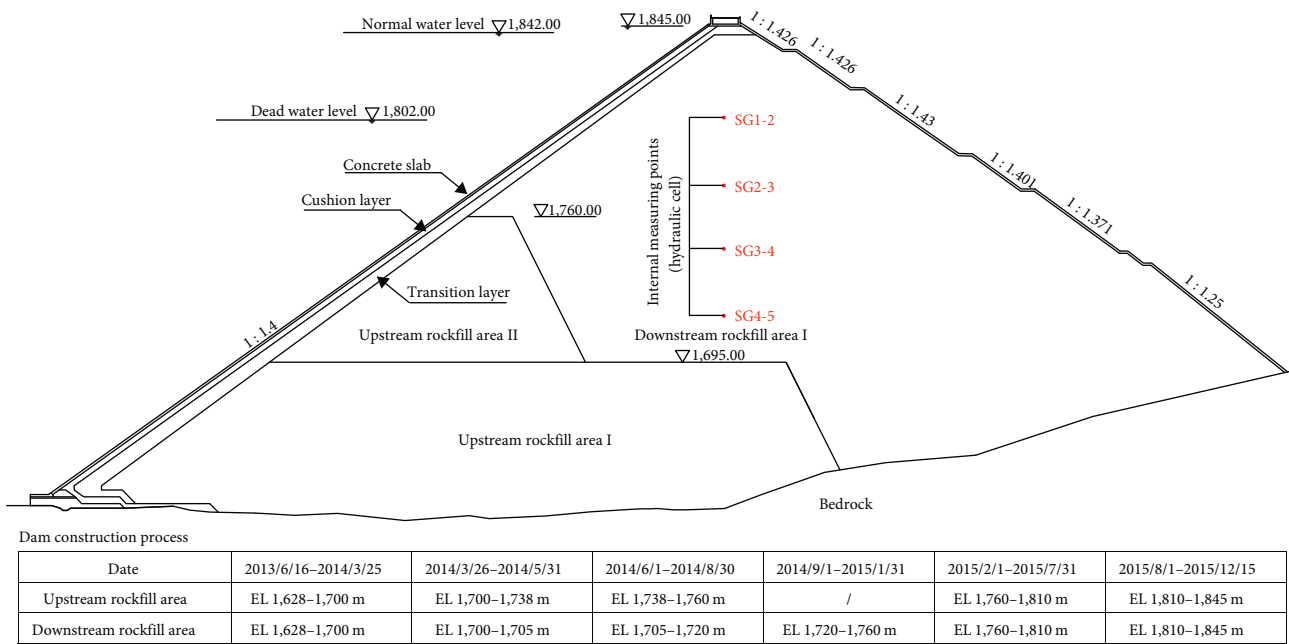
FIGURE 1: Typical cross-section and the construction process of the Houziyan dam.

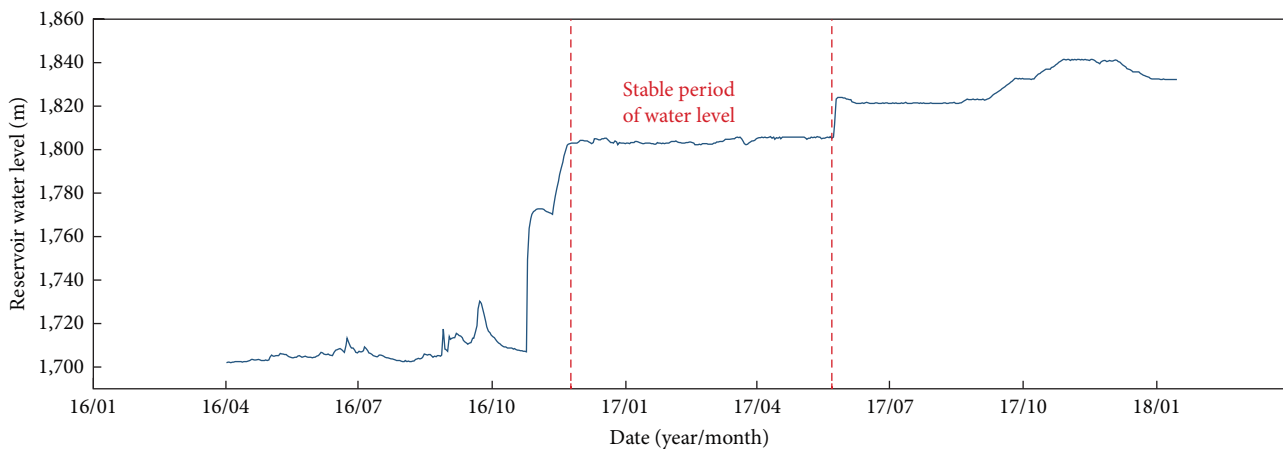| Date	2013/6/16–2014/3/25	2014/3/26–2014/5/31	2014/6/1–2014/8/30	2014/9/1–2015/1/31	2015/2/1–2015/7/31	2015/8/1–2015/12/15
Upstream rockfill area	EL 1,628–1,700 m	EL 1,700–1,738 m	EL 1,738–1,760 m	/	EL 1,760–1,810 m	EL 1,810–1,845 m
Downstream rockfill area	EL 1,628–1,700 m	EL 1,700–1,705 m	EL 1,705–1,720 m	EL 1,720–1,760 m	EL 1,760–1,810 m	EL 1,810–1,845 m

FIGURE 2: Water storage process of the studied project.

area is a narrow, V-shaped valley with bedrock primarily consisting of medium-thick to thick Lower Devonian dolomitic limestone and metamorphic limestone. The maximum thickness of the riverbed cover layer at the dam site is 75.2 m, which is a multilayer structure, with sand and gravel layers in the upper and lower parts and a clayey silt layer in the middle, which can be up to 29.5 m thick. To avoid problems of uneven deformation, permeability stability, and seismic liquefaction, the riverbed cover along the axis of the dam was completely excavated before the dam construction. In addition, the bedrock was reinforced by consolidation grouting to a depth of 10–35 m and no regional faults passed through the dam site area.

Figure 2 shows the water storage process of the Houziyan dam; it can be found that from November 15, 2016, to December 15, 2016, the reservoir rapidly stored water to the dead level (EL 1,802 m), and after a stable period of half a year, the water

level slowly rose and reached the normal storage level (EL 1,842 m) on November 20, 2017.

2.2. Finite Element Model. Based on the typical cross-section of the dam, a numerical model was established, as shown in Figure 3. The elements are first meshed in a 2D plane, then stretched into a 3D model with a width of 12 m, which is consistent with the actual width of a single concrete slab, and the number of nodes and elements are 4,984 and 2,379, respectively. In addition, since the geological conditions of the Houziyan CFRD are relatively favorable, the dam foundation can be considered an intact rock body in the numerical simulation.

Following the actual construction and reservoir storage process, the simulation of the dam body filling and slab-pouring process of the Houziyan CFRD is divided into 68 load steps. The hydrostatic load is applied directly on the
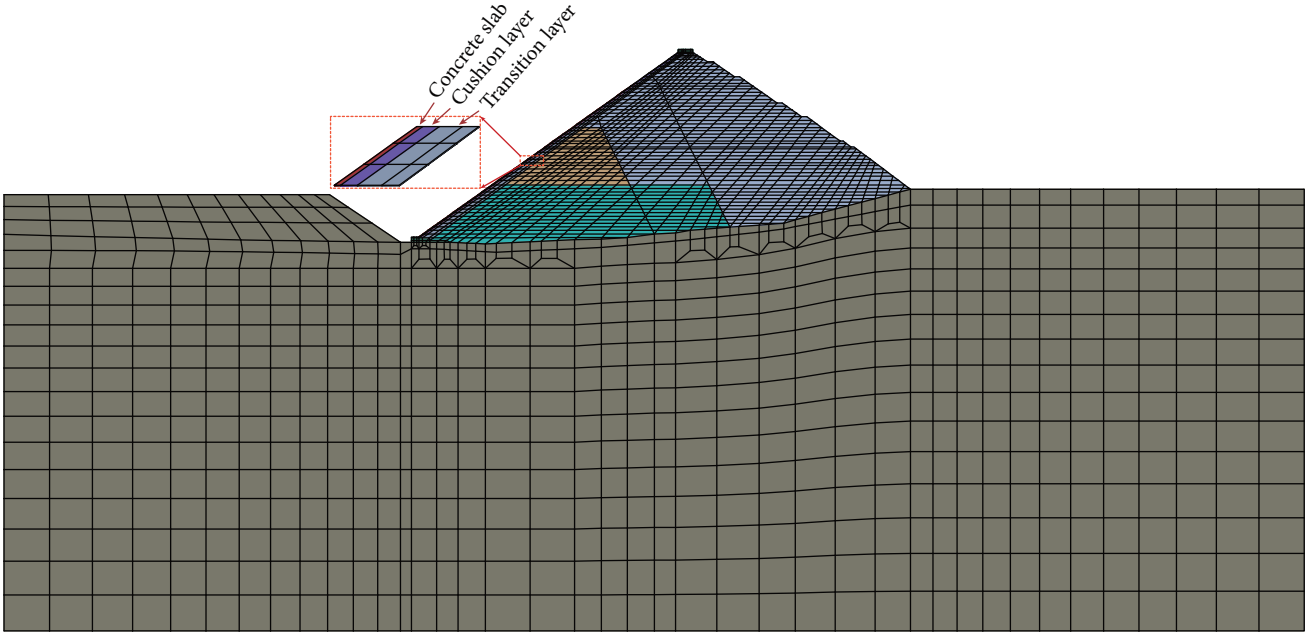
FIGURE 3: Numerical simulation model of the Houziyan dam.

slab, and 11 loading steps are used to simulate the reservoir water storage process, as shown in Figure 2. It should be noted that the coupled effects of seepage and deformation are not considered in this study, since the concrete slab of CFRDs can be considered completely impermeable structures, and the seepage through the dam body is neglected.

3. Methodology

3.1. Numerical Simulation and Parameter Calibration

3.1.1. The Constitutive Model. To investigate the operating characteristics of the CFRD and calculate the time-dependent reliability of the concrete slab, the numerical simulation of the CFRD at different periods is needed, including dam filling, slab construction, water storage, and subsequent operation. During the periods mentioned earlier, the dam will produce instantaneous deformation due to deadweight load and water load and time-dependent deformation due to the creep effect.

Duncan and Chang's E–B model, which is a nonlinear elastic model, is used to simulate the instantaneous deformation of the dam body under gravity and water loads. In this model, the tangent elastic modulus E and bulk modulus B are related to the stress state of the soil, which can be expressed as follows [32]:

$$E = K_e P_a \left(\frac{\sigma_3}{P_a}\right)^n \left(1 - R_f \cdot \frac{(\sigma_1 - \sigma_3)(1 - \sin\varphi)}{2c\cos\varphi + 2\sigma_3\sin\varphi}\right)^2, \quad (1)$$

$$B = K_b P_a \left(\frac{\sigma_3}{P_a}\right)^m, \quad (2)$$

where P_a is atmospheric pressure ($P_a = 101.4$ kPa); K_e, n, K_b, m, and R_f are parameters that can be determined from laboratory tests; c is the cohesion, and φ is the friction angle

considering the modification of the confinement pressure, given by Wei et al. [33]:

$$\varphi = \varphi_0 - \Delta\varphi \lg(\sigma_3/P_a). \quad (3)$$

The creep deformation is simulated with a seven-parameter creep, which considers that the creep deformation of rockfill material exhibits an exponential relationship with time as follows:

$$\varepsilon(t) = \varepsilon_f(1 - e^{-\alpha t}), \quad (4)$$

where $\varepsilon(t)$ is the creep deformation at time t; ε_f is the final creep deformation when $t \to \infty$; α is the ratio between the first day's creep and ε_f. The creep deformation for earth dams includes two parts, the volume creep deformation ε_{vf} and the shear creep deformation ε_{sf}, given by the following:

$$\varepsilon_{vf} = b_f \left(\frac{\sigma_3}{P_a}\right)^{m_1} + c_f \left(\frac{\sigma_1 - \sigma_3}{P_a}\right)^{m_2}, \quad (5)$$

$$\varepsilon_{sf} = d_f \left(\frac{SL}{1 - SL}\right)^{m_3}, \quad (6)$$

where b_f, c_f, d_f, m_1, m_2, and m_3 are parameters of the creep model.

3.1.2. Calibration of Parameters. For reliability analysis, the random parameters must be determined first. The distribution type and standard deviation of random parameters can be confirmed according to references. However, the mean value of random parameters needs to be calibrated for an actual project. The material mechanical parameters of the dam rockfill are mainly determined by indoor experiments

and the engineering analogy method. Due to the limitation of experiments and analogy, the obtained material parameters are difficult to accurately characterize the mechanical characteristics of the dam after completion [34, 35]. To make the numerical simulation more accurate and credible, the deformation back analysis of unknown parameters should be performed first.

The back analysis based on in-situ monitoring data is an effective method for calibrating the parameters of rockfill dams [36]. In this study, the RSM is used as a surrogate model for numerical analysis, and the objective functions for deformation back analysis can be expressed as follows:

$$F_{\text{obj}}(\theta) = \sum_i^q \sum_j^w \frac{1}{qw} \left(\frac{\delta_i(t_j)}{\delta_i^*(\theta, t_j)} \right), \tag{7}$$

where $F_{\text{obj}}(\theta)$ is the objective function with parameter combination θ; q is the number of measuring points, and w is the number of time points chosen for the analysis; $\delta_i(t_j)$ and $\delta_i^*(\theta, t_j)$ are the measured deformations and the calculated deformation of measuring point i at time j, respectively.

Parameter back analysis can be transformed into a mathematical optimization problem and the calibrated parameters $\tilde{X}$ are the combinations of parameters that minimize the objective function, i.e., $\tilde{X} = \text{argmin}\, F_{\text{obj}}(X)$. Different from the abovementioned research, the whale optimization algorithm (WOA) is used to get the optimal parameters in this study. WOA is an advanced optimization algorithm proposed by Mirjalili and Lewis [37]; compared with traditional optimization algorithms, such as genetic algorithm and particle swarm optimization algorithm, WOA has higher optimization accuracy and faster convergence speed [38]. The MATLAB codes of the WOA algorithm can be found in Mirjalili's paper [37].

3.2. Time-Dependent Fuzzy Reliability Analysis

3.2.1. Formulation of Time-Dependent Fuzzy Reliability Analysis. Reliability represents the ability of a structure to resist external loadings under the influence of uncertainties and is usually defined by the performance function $g(\mathbf{X})$, where $\mathbf{X} = \{x_1, x_2, \ldots, x_n\}$ is a vector containing an n-dimensional random variable. During the CFRD water storage process, the safety performance of the concrete slab varies with the evolution of load (e.g., the hydrostatic pressure) and the development of dam body deformation, and in contrast to deterministic reliability analysis, the performance function of the concrete slab in this situation exhibits time-dependent characteristics that can be expressed as $g(\mathbf{X}, t)$, and $g(\mathbf{X}, t) \leq 0$ denotes the instantaneous failure at time t. Assuming that $f(\mathbf{X}) = f(x_1, x_2, \ldots, x_n)$ represents the joint probability density function (PDF) of $\mathbf{X}$, then the expression of the time-dependent failure probability is as follows:

$$P_f(t) = \int_{\Omega_{F,t}} f(\mathbf{X}) d\mathbf{X} = \int_{-\infty}^{\infty} I[g(\mathbf{X}, t)] f(\mathbf{X}) d\mathbf{X}, \tag{8}$$

where $\Omega_{F,t} = \{x | g(\mathbf{X}, t) \leq 0\}$ indicates the failure domain; $I[g(\mathbf{X}, t)]$ is an indicator function, under the deterministic failure criteria, $I[g(\mathbf{X}, t)] = 1$, if $\mathbf{X} \in \Omega_{F,t}$, and $I[g(\mathbf{X}, t)] = 0$ otherwise. However, in practical engineering, there is no strict and precise threshold limit for slab cracking, i.e., the failure criteria have certain fuzzy features. In this study, the small form of the Semiridged membership function is introduced to describe the fuzzy failure criteria of concrete slab cracking as follows [30, 39]:

$$I[g(\mathbf{X}, t)] = u[g(\mathbf{X}, t)] = \begin{cases} 1 & g(\mathbf{X}, t) \leq a \\ \dfrac{1}{2} - \dfrac{1}{2} \sin \dfrac{\pi}{b-a} \left[g(\mathbf{X}, t) - \dfrac{a+b}{2} \right] & a < g(\mathbf{X}, t) < b, \\ 0 & g(\mathbf{X}, t) \geq b \end{cases} \tag{9}$$

where $u[g(\mathbf{X}, t)]$ is the membership function of the performance function, and a and b are the lower and upper limits of fuzzy intervals. The general formulation of time-dependent fuzzy reliability analysis can be established by introducing Equation (9) into Equation (8).

3.2.2. Time-Dependent Performance Functions. The operating environment of a CFRD is very complex; under the effect of the reservoir water, the hydrostatic load is transferred to the dam body through the concrete slab, and the stresses in the slab are influenced by the hydrostatic load, gravity, and the contact action with the rockfill area. At higher stress states, tensile damage and plastic-yielding damage may easily lead to slab cracking [4]. As we know, the deformation and stress of the concrete slab evolve with the operation of the CFRD, resulting in the time-dependent characteristics of its reliability.

Assuming that the tensile stress of the concrete slab at time t is $\sigma_{\text{ten}}(t)$, Under the tensile strength criterion, the performance function based on the tensile strength criterion at time t can be expressed as the difference between the tensile strength of the concrete R_c and the tensile stress of the slab $\sigma_{\text{ten}}(\mathbf{X}, t)$.

$$g_{\text{ten}}(\mathbf{X}, t) = R_c - \sigma_{\text{ten}}(\mathbf{X}, t). \tag{10}$$

The time-dependent performance functions based on the DP yield criterion can be expressed as follows:
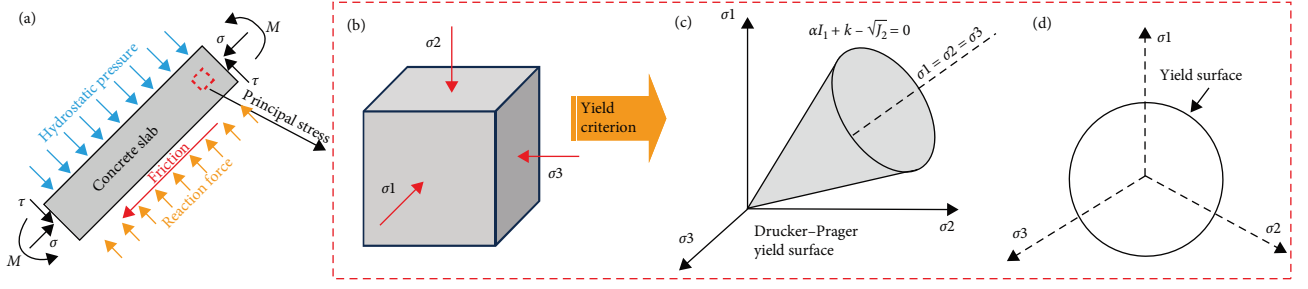
FIGURE 4: Diagram of the Drucker–Prager yield criterion: (a) the loads acting on the concrete slab, (b) the microelement subjected to three-directional principal stresses, (c) the Drucker–Prager yield surface in 3D space of principal stresses, and (d) the Drucker–Prager yield surface in π plane.

$$g_{DP}(\mathbf{X}, t) = \alpha I_1(\mathbf{X}, t) + k - \sqrt{J_2(\mathbf{X}, t)}, \tag{11}$$

with,

$$I_1(\mathbf{X}, t) = \sigma_1(\mathbf{X}, t) + \sigma_2(\mathbf{X}, t) + \sigma_3(\mathbf{X}, t), \tag{12}$$

$$J_2(\mathbf{X}, t) = \frac{1}{6} \sum_{i<j} \left[\sigma_i(\mathbf{X}, t) - \sigma_j(\mathbf{X}, t) \right]^2 \quad i, j = 1, 2, 3, \tag{13}$$

where σ_i ($\mathbf{X}$, t), $i = 1, 2, 3$ are the principal stresses at time t; α and k are constants parameters that reflect the strength of the material, which have the following conversion relation with the cohesion c and internal friction φ of Mohr–Coulomb yield criterion:

$$\alpha = \frac{\sin \varphi}{\sqrt{3}\sqrt{3 + \sin^2 \varphi}}, \tag{14}$$

$$k = \frac{3c \cos \varphi}{\sqrt{3}\sqrt{3 + \sin^2 \varphi}}. \tag{15}$$

During the operation of CFRDs, the loads acting on the concrete slab mainly include the hydrostatic pressure, the restraining action of the upper and lower sections, and the reaction and friction forces of the overlying soil, see Figure 4(a). For a microelement located in the concrete slab subjected to three-directional principal stresses (Figure 4(b)), the magnitude and ratio of the principal stresses will inevitably change as the load on the slab increases, and if it exceeds the yield surface of the DP criterion (see Figures 4(c) and 4(d)), the material will be yielded to damage, thereby the cracking of the concrete slab.

As shown in Equations (10) and (11), the performance functions are related to the strength and the stress state of the concrete slab, while the latter depends on the random mechanical parameters of the dam body and slab. Given the complexity of the CFRD structure and the constitutive model, it is impractical to apply time-consuming numerical simulations directly to the reliability analysis process. The surrogate model (also known as the meta-model) is an effective tool to solve this problem, which is applied to infer the inputs/outputs mapping relationships [3, 40]. In this study, the RSM is used as the surrogate model to reconstruct

performance functions with the following expressions:

$$g_{ten}(\mathbf{X}, t) = R_c - \left(\sum_{i=1}^{n} a_i^t x_i + \sum_{i=1}^{n} b_i^t x_i^2 + c_1^t \right), \tag{16}$$

$$g_{DP}(\mathbf{X}, t) = \sum_{i=1}^{n} d_i^t x_i + \sum_{i=1}^{n} e_i^t x_i^2 + c_2^t, \tag{17}$$

where $\{a_i^t, b_i^t, d_i^t, e_i^t\}$ ($i = 1, 2, \ldots, n$), and c_1^t, c_2^t are coefficients, which can be determined by multivariate statistical regression.

3.2.3. MCS for Fuzzy Reliability Analysis. Compared to analytical algorithms such as the FOSM method, the MCS, which estimates the failure probability of structures through random sampling, is considered to be a more effective and accurate method [40, 41]. Under the deterministic failure criteria, according to the joint PDF $f(\mathbf{X})$, each basic random variable x_i is randomly sampled and substituted into the RSM function. The number of times that $g(\mathbf{X}, t) < 0$ is recorded as n_f, assuming that the total sampling number is N, the estimated failure probability can be calculated as follows [42]:

$$\widehat{P}_f(t) = \frac{n_f}{N}. \tag{18}$$

With considering the fuzzy feature of the failure criterion, whether $g(\mathbf{X}, t) < 0$ or not, the membership function value calculated by Equation (9) is recorded, and the fuzzy failure probability is as follows:

$$\widehat{P}_f(t) = \frac{1}{N} \sum_{n=1}^{N} u\left[g\left(\mathbf{X}^{(n)}, t \right) \right]. \tag{19}$$

Given that the cracking accident is indicated by any part of the slab exceeding the strength limit state, the safety assessment of the concrete slab can be considered as a tandem system reliability issue, which can be calculated with the following formulation:
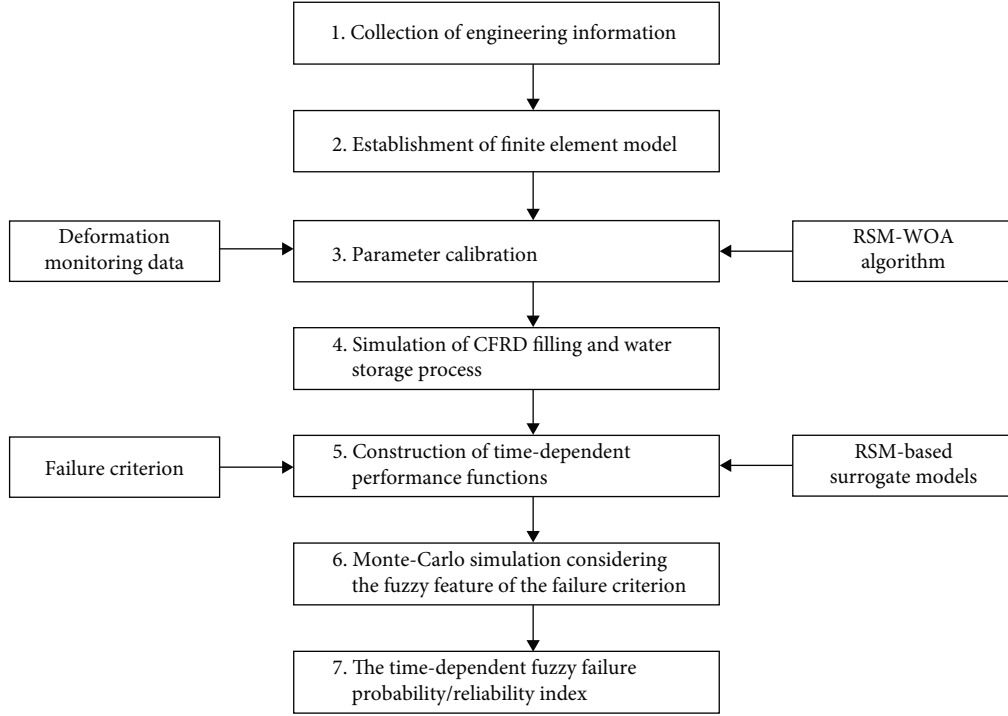
FIGURE 5: Implementation process of the proposed methodology.

$$\widehat{P}_f^s(t) = \frac{1}{N} \sum_{n=1}^{N} \max\left\{ u\left[g^k\left(\mathbf{X}^{(n)}, t\right)\right] \right\} \quad 1 \le k \le M, \qquad (20)$$

where M is the number of failure paths of the tandem system, which in this study is the product of the number of failure points and the failure modes. $g^k(\mathbf{X}^{(n)}, t)$ is the performance function corresponding to the kth failure path in the nth sampling of $\mathbf{X}$ at time t. To reduce the sampling error, the required sampling times should generally meet the requirements of $N \ge 100/\widehat{P}_f^s(t)$. Then, the corresponding time-dependent fuzzy reliability index can be defined by the inverse of the standard normal cumulative distribution function of the time-dependent failure probability:

$$\beta(t) = \Phi^{-1}\left(1 - \widehat{P}_f^s(t)\right), \qquad (21)$$

where $\Phi^{-1}(\cdot)$ is the inverse standard normal cumulative distribution function.

3.3. Implementation Procedures of the Proposed Method. The main objective of this paper is to investigate the fuzzy reliability of the concrete slab during the water storage period of the Houziyan CFRD. Figure 5 shows the basic framework and implementation process of the proposed method, and details of each step are given below:

Step 1: Collect engineering information, mainly including dam design information, engineering geological conditions, health monitoring data, etc.

Step 2: Establish the finite element model of the dam and foundation; it should be emphasized that corresponding nodes should be set at the location of the monitoring points for subsequent parameter calibration.

Step 3: Select appropriate constitutive models to simulate the stress-deformation state of the CFRD (Duncan and Chang's E–B model, the seven-parameter creep model, and the DP model are selected in this study), and calibrate the parameters based on the deformation monitoring data.

Step 4: Simulation of the filling and water storage process of the CFRD based on the established finite element model and calibrated parameters.

Step 5: According to the tensile strength criterion and the DP yield criterion, the time-dependent performance functions can be constructed with Equations (10) and (11), then transformed into the explicit form shown in Equations (16) and (17) using the RSM-based surrogate models.

Step 6: The SMF is utilized to describe the fuzzy failure criteria of concrete slab cracking, and then the MCS is performed according to the statistical characteristics of the random variables.

Step 7: Based on Equation (20), the time-dependent fuzzy failure probability of the concrete slab can be calculated, and the corresponding time-dependent fuzzy reliability index can also be obtained through Equation (21).

4. Results and Discussion

4.1. Parameters Calibration Based on Monitoring Data. To improve the fidelity and credibility of the numerical simulation of CFRDs during construction and the water storage

TABLE 1: Parameters calibration results of Duncan and Chang's E–B model.

Material	K_e	K_{ur}	m	R_f	K_b	φ_0 (°)	$\Delta\varphi$ (°)	n
Cushion and transition	1,312	1,283	0.35	0.62	559.2	49.3	2.7	0.36
Upstream rockfill	1,486	1,623	0.26	0.71	419.8	46.7	3	0.31
Downstream rockfill	1,055	1,489	0.32	0.68	530.3	44.2	3.2	0.28

TABLE 2: Parameters calibration results of seven-parameters creep model.

Material	α	b_f	c_f	d_f	m_1	m_2	m_3
Cushion and transition	5.7×10^{-3}	8.1×10^{-5}	1.52×10^{-4}	5.14×10^{-4}	0.68	0.41	0.55
Upstream rockfill	8.1×10^{-3}	5.5×10^{-5}	1.24×10^{-4}	4.92×10^{-4}	0.51	0.42	0.43
Downstream rockfill	7.2×10^{-3}	7.6×10^{-5}	1.39×10^{-4}	6.06×10^{-4}	0.41	0.37	0.48

TABLE 3: Adopted parameters of the Drucker–Prager model.

Material	E (GPa)	Poisson ratio	c (MPa)	φ (°)	R_c (MPa)	Density (kg/m^3)
Concrete slab	30	0.167	3.18	54.9	2	2,500

period, the calibration of the material parameters is performed based on the monitoring sequence at four measuring points, including SG1-2, SG2-3, SG3-4, and SG4-5, which monitor the settlement of dam body during dam filling and operation. These measuring points are all located on the dam axis, and the specific positions are also shown in Figure 1. RSM was utilized as the surrogate model to generate the objective function for parameter calibration according to Equation (7). Then, the parameter calibration problem is converted into an objective function optimization problem, and the WOA is applied to this process. Due to the multi-dimension of the parameters, the instantaneous deformation and creep deformation are decoupled in this study, and the creep parameters are calibrated first. As mentioned earlier, there is a 6-month water level stabilization period during the Houziyan dam impoundment, i.e., from December 15, 2016, to June 15, 2017. The observed monitoring data during this period can be considered to reflect the deformation caused by creep effects, which can be used as the data source for calibrating creep parameters. Then, the determined creep parameters are fixed, and the Duncan–Chang parameters are calibrated in the same way based on the full sequence of deformation data. The calibrated parameters are listed in Tables 1 and 2, and it should be noticed that the DP model parameters of concrete slabs adopt the test values which are listed in Table 3.

The calibrated parameters are adopted to simulate the deformation and stress of the Houziyan CFRD, and the contours of the displacement, when the dam filling process is completed, are shown in Figure 6, which includes the settlement and horizontal directions. It can be seen that the maximum settlement of the dam is 1.56 m, less than 1% of the dam height, and the maximum horizontal displacement is also in the normal range, which is 0.26 and 0.1 m in the upstream and downstream directions, respectively. The numerical simulation results show that the deformation of

the Houziyan dam is relatively normal and consistent with the deformation law of earth dams.

The measured and computed settlement sequence of the monitoring points SG1-2, SG2-3, SG3-4, and SG4-5 are compared in Figure 7. It can be seen that the calculated settlement and the measured settlement are in good agreement. In this study, three prediction performance indicators, root mean square error (RMSE), mean absolute error (MAE), and mean absolute percentage error (MAPE), are adopted to evaluate the simulation error of calibrated parameters, and the calculation formulas can be expressed as follows:

$$\text{MAE} = \frac{1}{w} \sum_{j=1}^{w} \left| \delta(t_j) - \delta^*(\theta, t_j) \right|, \tag{22}$$

$$\text{RMSE} = \sqrt{\frac{1}{w} \sum_{j=1}^{w} \left[\delta(t_j) - \delta^*(\theta, t_j) \right]^2}, \tag{23}$$

$$\text{MAPE} = \frac{100\%}{w} \sum_{j=1}^{w} \left| \frac{\delta(t_j) - \delta^*(\theta, t_j)}{\delta(t_j)} \right|, \tag{24}$$

where w is the number of time points chosen for the analysis; $\delta(t_j)$ and $\delta^*(\theta, t_j)$ are the measured deformation and the calculated deformation at time j, respectively.

The results of the error evaluation are listed in Table 4, it can be seen that the numerical simulation using calibrated parameters has a higher accuracy, with the MAPE less than 6%. To sum up, the numerical simulation can well predict the deformation characteristics during dam filling and water storage, and the calibrated parameters can be regarded as the mean value of random parameters.

4.2. Time-Dependent Fuzzy Reliability Analysis of the Concrete Slab. In the reliability analysis of dam structures, the random factors that are easier to control and measure (e.g., density,

YDISP (mm): −1,500 −1,400 −1,300 −1,200 −1,100 −1,000 −900 −800 −700 −600 −500 −400 −300 −200 −100

(a)

XDISP (mm): −260 −240 −220 −200 −180 −160 −140 −120 −100 −80 −60 −40 −20 0 20 40 60 80
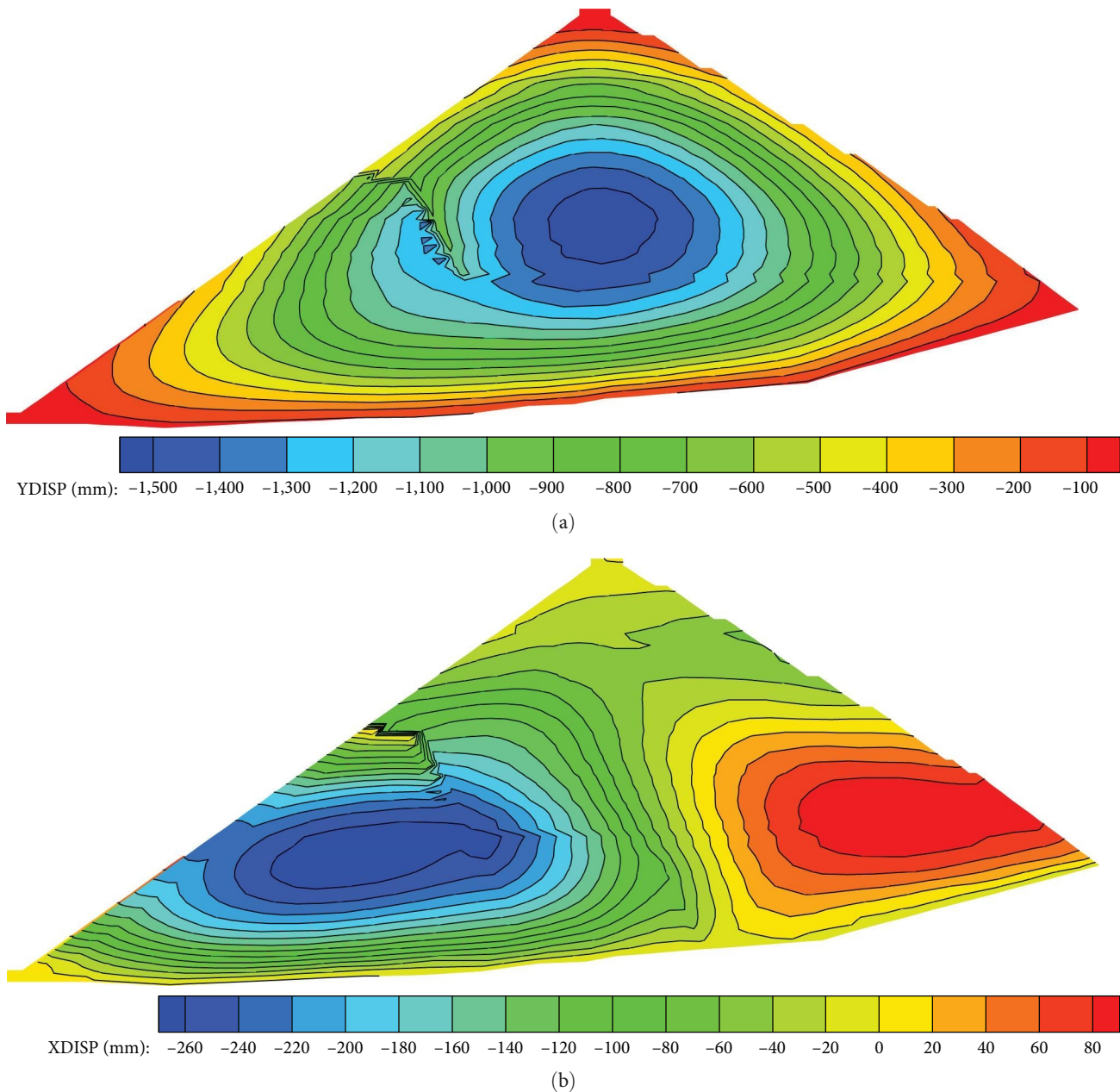
(b)

FIGURE 6: The deformation contour of the Houziyan dam at the moment of completion: (a) settlement deformation and (b) horizontal deformation.

structural size, etc. [18, 27]) or have less impact on structural safety (e.g., Poisson ratio, etc. [43]), are generally not considered. In addition, the reservoir water level is also an important factor that affects the reliability of the concrete slab. However, in time-dependent reliability analysis, the hydrostatic pressure applied to the numerical model is determined based on the observed water level sequence, which does not have a random character, and its influence will be reflected in the evolution of reliability. The random variables and their distribution characteristics are determined based on existing studies [18, 27], as listed in Table 5.

The cracking of the slab at any position implies damage to the overall structure. To estimate the system reliability index of the concrete slab, several feature points are chosen

by different elevations, as shown in Figure 8. It should be noted that Hu et al. [25] pointed out that the construction seams of concrete slabs are more prone to cracking, so the locations of feature point 3 and feature point 8 were set at the construction seam of phases I and II slab (EL 1,695 m) and that of phases II and III slab (EL 1,797 m), respectively.

The positive and negative stresses in the numerical simulation represent the compressive and tensile stresses, respectively. Therefore, the third principal stress represents the maximum tensile stress state that occurs in the concrete slab, and its contour is shown in Figure 9(a). We can find that a larger tensile stress state of about 1.5 MPa appears in the upper part of the slab, close to the elevation of characteristic point 8, which indicates that the cracking caused by

(a)   (b)
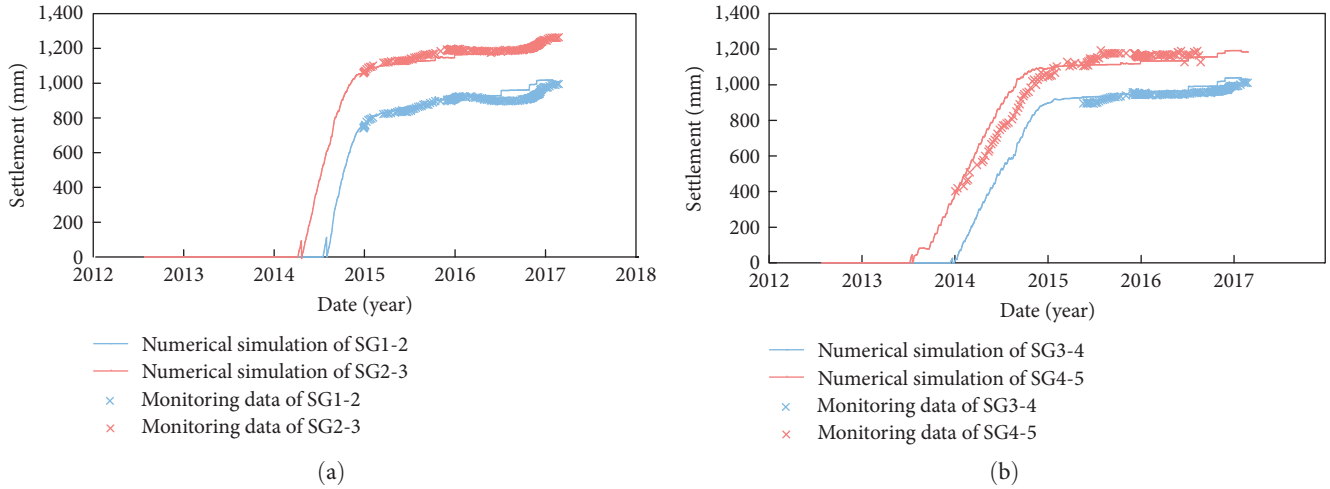
FIGURE 7: Comparison of observed deformation and simulation results: (a) SG1-2 and SG2-3, (b) SG3-4 and SG4-5.

TABLE 4: Numerical simulation error assessment of calibrated parameters.

Performance indicator	SG1-2	SG2-3	SG3-4	SG4-5
RMSE (m)	42.45	24.85	34.45	66.69
MAE (m)	32.46	21.23	28.69	53.89
MAPE (m)	3.36%	1.81%	2.87%	5.51%

TABLE 5: Distribution characteristics of random factors.

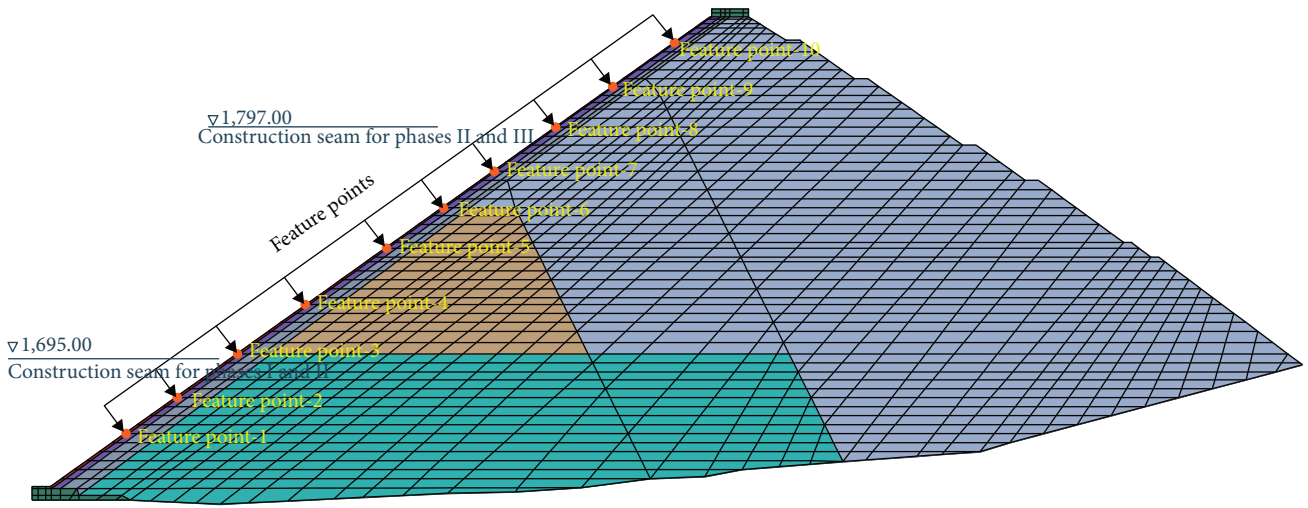| Material	Random factors	Mean	Coefficient of variation	Distribution type
Upstream rockfill	$\tan \varphi_1$ (°)	1.06	0.1	Normal
Downstream rockfill	$\tan \varphi_2$ (°)	0.97	0.1	Normal
Concrete slab	c (MPa)	3.18	0.1	Normal
	$\tan \varphi_3$ (°)	1.42	0.1	Normal
	E (GPa)	30	0.1	Normal

FIGURE 8: Location of the selected feature points in the numerical model.
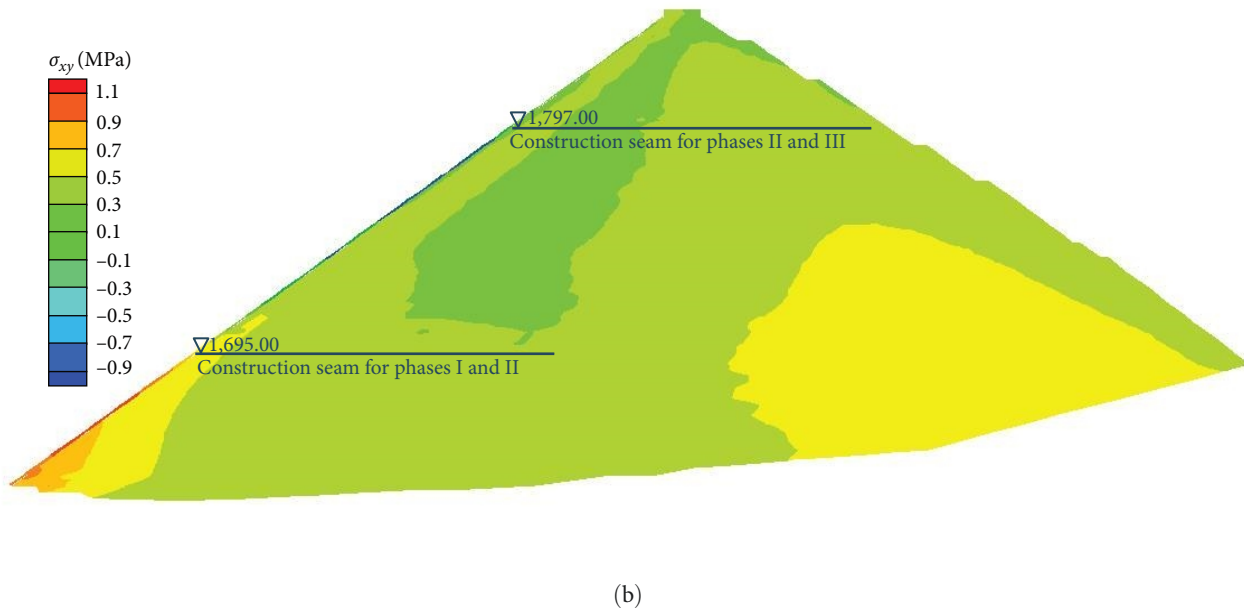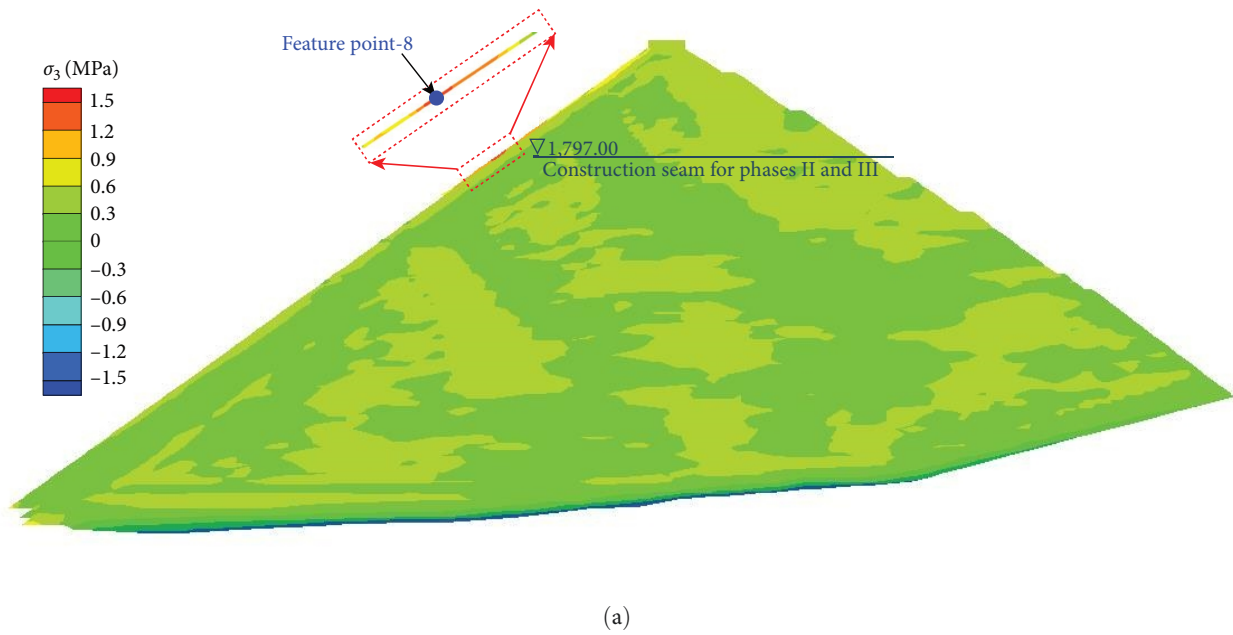
(a)

(b)

FIGURE 9: The stress contour of the Houziyan dam at normal water level: (a) tensile stress (third principal stress) and (b) shear stress.

tension is more likely to occur at the construction seam of the second and third phase slabs. Figure 9(b) is the contour of shear stress, and it can be seen that relatively large shear stresses with values of 1.1 and −0.9 MPa appear near the two construction seams, respectively. The reason for the high-stress state at the construction seams may be that the slabs are not poured at one time. When the lower slabs are poured, the dam body continues to deform, and the uneven deformation of the slabs and the rockfill part at the construction seams is generated when the new slabs are poured.
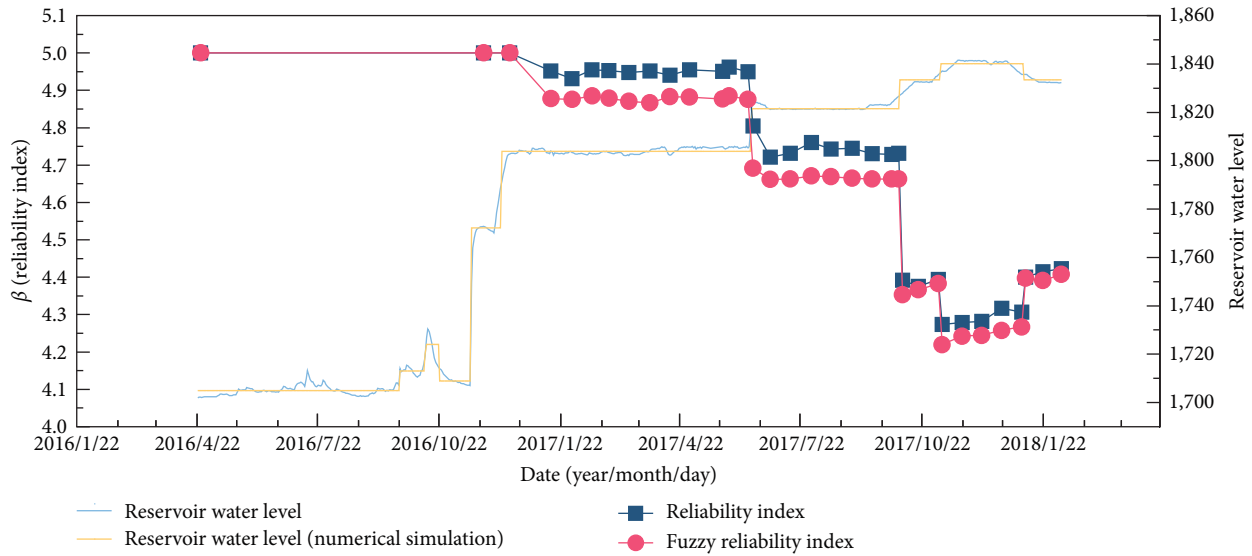
FIGURE 10: The time-dependent fuzzy reliability index and the time-dependent reliability index without considering fuzzy failure criteria.

For each feature point in the concrete slab, two failure types are considered, and a series system containing 20 failure paths can be constructed. The initial water storage period of the Houziyan CFRD lasted from April 23, 2016, to February 5, 2018, and 34 moments were selected for reliability analysis. Based on the statistical characteristics (mean and coefficient of variation) listed in Table 4, the random variables are divided into three levels with a fluctuation range of 3σ. Fifteen sets of variable combinations are generated using the orthogonal design method, and the corresponding numerical simulations are performed to extract the stress states of each feature point at each moment point. The coefficients of Equations (16) and (17) (i.e., the RSM of g_{ten} (**X**, t) and g_{DP} (**X**, t)) are fitted using statistical regression. The complex correlation coefficients R^2 are adopted to evaluate the accuracy of the RSM model, and the fitting results showed that the R^2 of the RSM equation at each moment for each feature point is higher than 0.85, meeting the accuracy requirements of the surrogate model in the reliability analysis. Combining the established RSM model and MCS, the fuzzy system failure probability at each time during the water storage period can be estimated according to Equation (20) and the corresponding time-dependent fuzzy reliability index is calculated by Equation (21).

Figure 10 shows the reliability index sequence of the concrete slab during the initial reservoir storage period. Generally, with the increasing reservoir water level, the fuzzy reliability index of the concrete slab tends to decrease, ranging from 4.22 to 5.0. When the reservoir water level is below the dead level (1,802 m), the fuzzy reliability index remains at 5, implying that there is no risk of slab cracking during this time. The cracking risk of the panels is also relatively low when the reservoir level is stabilized at the dead level, and the fuzzy reliability index is between 4.85 and 4.90. After that, the fuzzy reliability index decreases significantly with the rapid rise of the reservoir level and drops to the lowest level of 4.22 after the reservoir level reaches the normal water level

(1,842 m). It is worth noting that as the reservoir level stabilizes, the reliability index tends to rise slowly, although the magnitude is not significant; it also reflects that the deformation between the slab and the dam body is gradually coordinated, and the stress level is gradually reduced under a stable load.

In contrast, the system reliability index without considering fuzzy failure criteria is also shown in Figure 10, with data from the study of Li et al. [27]. Compared with the fuzzy reliability index, the reliability index is improved when the fuzziness of the failure criterion is not considered, with a maximum amplitude of 2.34% and an average amplitude of 1.23%. This is because when Monte-Carlo sampling is carried out, the sampling points located in the fuzzy interval are more located on the side where the performance function is greater than 0, and these sampling points are regarded as safe points when the fuzzy failure criterion is not considered. In the unified standard for the reliability design of hydraulic engineering structures (GB50199-2013) of China, it is stipulated that the reliability index of the dam structure should be higher than 4.2. In general, the safety performance of the concrete slab of the Houziyan CFRD satisfies this standard, but the operational state of the slab should be monitored carefully in the long-term operation.

5. Conclusions

In this paper, a time-dependent reliability analysis method considering the fuzziness of the failure criterion is proposed, and the safety state of the concrete slab of the Houziyan CFRD during the initial water storage period is investigated. The results show the following:

(1) The instantaneous and creep parameters of Houziyan CFRD are calibrated by the RSM-WOA method, and the MAPE between the measured and the deformation calculated using the calibrated parameters is less than 6%. It shows that the adopted numerical

model and parameters have high accuracy, which provides the basis for the subsequent reliability analysis.

(2) The fuzzy reliability index of concrete slabs decreases with the rise of reservoir water level, representing that higher hydrostatic loads are more likely to lead to slab cracking and vice versa. When the reservoir water level is relatively stable, the deformation of the slab and the dam body tend to be coordinated, and the safety performance of the concrete slab will be slightly improved. When the reservoir first reaches its normal storage level, the fuzzy reliability indicator is the lowest at 4.22.

(3) The reliability analysis results considering and without considering the fuzziness of the failure criterion are compared. Without considering the fuzzy failure criterion, the time-dependent reliability trend remains unchanged, but the reliability index increases slightly. From a conservative point of view, in the reliability-based design of concrete slabs, it is more beneficial to structural safety to consider the fuzziness of the failure criterion.

This study can help researchers and engineers evaluate the safety performance of the concrete slab of CFRDs during the initial water storage period. The fuzzy reliability-based optimization methods for CFRD construction and water storage scheduling may be a future research direction.

Abbreviations

B: Bulk modulus
CFRD: Concrete-faced rockfill dam
c: Cohesion
DP: Drucker–Prager
E: Tangent elastic modulus
ε_f: Final creep deformation
ε_{vf}: Final volume creep deformation
ε_{sf}: Final shear creep deformation
$f(\cdot)$: Joint probability density function
$F_{obj}(\cdot)$: Objective function for parameter calibration
$g(\cdot)$: Performance function
$I(\cdot)$: Indicator function
I_1: First stress invariable
J_2: Second deviatoric stress tensor invariable
MAE: Mean absolute error
MAPE: Mean absolute percentage error
n: Number of random variables
P_a: Atmospheric pressure
PDF: Probability density function
$P_f(\cdot)$: Failure probability
$\widehat{P}_f(\cdot)$: Fuzzy failure probability
$\widehat{P}_f^s(\cdot)$: Fuzzy failure probability of tandem system
q: Number of measuring points
R_c: Tensile strength of the concrete
RMSE: Root mean square error
RSM: Response surface method
$u(\cdot)$: Membership function
w: Number of time points

WOA: Whale optimization algorithm
$\mathbf{X}$: An n-dimensional vector of random variables
$\tilde{X}$: Parameter combination that minimizes the objective function
$\beta(\cdot)$: Fuzzy reliability index
$\delta_i(\cdot)$: Measured deformation
$\delta_i^*(\cdot)$: Calculated deformation
θ: Parameter combination
σ_1: Maximum principal stress
σ_2: Medium principal stress
σ_3: Minimum principal stress
$\sigma_{ten}(\cdot)$: Tensile stress
φ: Internal friction angle
$\Phi^{-1}(\cdot)$: Inverse standard normal cumulative distribution function
$\Omega_{F,t}$: Failure domain at time t.

Data Availability

The data that support the findings of this study are available from the corresponding author upon reasonable request.

Conflicts of Interest

The authors declare that they have no conflicts of interest regarding the publication of this paper.

Acknowledgments

References

[1] J. B. Cooke, "Development of the high concrete faced rockfill dam," *International Water Power and Dam Construction*, vol. 44, no. 4, pp. 7–9, 1992.

[2] H. Ma and F. Chi, "Technical progress on researches for the safety of high concrete-faced rockfill dams," *Engineering*, vol. 2, no. 3, pp. 332–339, 2016.

[3] M. E. Kartal, A. Bayraktar, and H. B. Başağa, "Nonlinear finite element reliability analysis of concrete-faced rockfill (CFR) dams under static effects," *Applied Mathematical Modelling*, vol. 36, no. 11, pp. 5229–5248, 2012.

[4] H. Q. Ma and K. M. Cao, "Key technical problems of extra-high concrete faced rock-fill dam," *Science in China Series E: Technological Sciences*, vol. 50, pp. 20–33, 2007.

[5] J. Zhou, J. Wei, T. Yang, P. Zhang, F. Liu, and J. Chen, "Seepage channel development in the crown pillar: insights from induced microseismicity," *International Journal of Rock Mechanics and Mining Sciences*, vol. 145, Article ID 104851, 2021.

[6] O. Azeez, A. Elfeki, A. S. Kamis, and A. Chaabani, "Dam break analysis and flood disaster simulation in arid urban environment: the Um Al-Khair dam case study, Jeddah, Saudi Arabia," *Natural Hazards*, vol. 100, pp. 995–1011, 2020.

[7] W. Wang, W. Chen, and G. Huang, "Research on flood propagation for different dam failure modes: a case study in Shenzhen, China," *Frontiers in Earth Science*, vol. 8, Article ID 527363, 2020.

[8] S. Cui, X. Pei, Y. Jiang et al., "Liquefaction within a bedding fault: understanding the initiation and movement of the Daguangbao landslide triggered by the 2008 Wenchuan Earthquake (Ms = 8.0)," *Engineering Geology*, vol. 295, Article ID 106455, 2021.

[9] W. Ma, G. Zhang, Y. Yang, P. Wang, Y. Zhao, and Q. Lin, "The piping failure mechanism of a loess dam: the 2021 dam break of the Yang Village Reservoir in China," *Frontiers in Earth Science*, vol. 10, Article ID 892179, 2022.

[10] H. Li, Y. He, Q. Xu, J. Deng, W. Li, and Y. Wei, "Detection and segmentation of loess landslides via satellite images: a two-phase framework," *Landslides*, vol. 19, pp. 673–686, 2022.

[11] Z. Wu, C. Chen, X. Lu, L. Pei, and L. Zhang, "Discussion on the allowable safety factor of slope stability for high rockfill dams in China," *Engineering Geology*, vol. 272, Article ID 105666, 2020.

[12] L. Wang, C. Wu, Z. Yang, and L. Wang, "Deep learning methods for time-dependent reliability analysis of reservoir slopes in spatially variable soils," *Computers and Geotechnics*, vol. 159, Article ID 105413, 2023.

[13] Y. Fang, C. He, Y. Su, K. Feng, and Z. He, "Supplement to the reliability index approach and its application to tunnel reliability problems," *Computers and Geotechnics*, vol. 163, Article ID 105767, 2023.

[14] C. Zhang, W. Li, D. Liu et al., "Seismic reliability research of continuous girder bridge considering fault-tolerant semi-active control," *Structural Safety*, vol. 102, Article ID 102322, 2023.

[15] T. Z. Zheng, W. Q. Wang, X. X. Li, W. G. Luo, and J. K. Chen, "Slope stability and reliability of kajiwa concrete-face rockfill dam using nonlinear strength parameters," *Journal of Yangtze River Scientific Research Institute*, vol. 29, no. 6, pp. 68–73, 2012.

[16] Z. Y. Wu and J. K. Chen, "Reliability analysis of slope stability of concrete faced rockfill dam considering nonlinear strength parameters," *International Journal Hydroelectric Energy*, vol. 31, no. 9, pp. 72–75, 2013.

[17] M. E. Kartal, A. Bayraktar, and H. B. Başağa, "Seismic failure probability of concrete slab on CFR dams with welded and friction contacts by response surface method," *Soil Dynamics and Earthquake Engineering*, vol. 30, no. 11, pp. 1383–1399, 2010.

[18] Q. Wu, X. Yu, and K. Zhao, "Response surface method and its application in reliability analysis of concrete-faced rockfill dam," *Chinese Journal of Rock Mechanics and Engineering*, vol. 9, pp. 1506–1511, 2005.

[19] R. Pang, B. Xu, D. Zou, and X. Kong, "Stochastic seismic performance assessment of high CFRDs based on generalized probability density evolution method," *Computers and Geotechnics*, vol. 97, pp. 233–245, 2018.

[20] K. Chen, R. Pang, and B. Xu, "Stochastic dynamic response and seismic fragility analysis for high concrete face rockfill dams considering earthquake and parameter uncertainties," *Soil Dynamics and Earthquake Engineering*, vol. 167, Article ID 107817, 2023.

[21] Y. Lu, R. Pang, M. Du, and B. Xu, "Simulation of non-stationary ground motions and its applications in high concrete faced rockfill dams via direct probability integral method," *Engineering Structures*, vol. 298, Article ID 117034, 2024.

[22] Y. Liu, D. Zheng, E. Cao, X. Wu, and Z. Chen, "Cracking risk analysis of face slabs in concrete face rockfill dams during the operation period," *Structures*, vol. 40, pp. 621–632, 2022.

[23] J. Yang, L. Pei, C. Kuang, Y. Li, and Y. Liu, "Dynamic evaluation method for Time-variant reliability of structural

[24] M. S. Won, H. J. Kim, and Y. C. Jung, "A study on the face slab deformation of concrete faced rockfill dams during initial impoundment," *KSCE Journal of Civil and Environmental Engineering Research*, vol. 35, no. 1, pp. 129–139, 2015.

[25] K. Hu, J. Chen, and D. Wang, "Shear stress analysis and crack prevention measures for a concrete-face rockfill dam, advanced construction of a first-stage face slab, and a first-stage face slab in advanced reservoir water storage," *Advances in Civil Engineering*, vol. 2018, Article ID 2951962, 10 pages, 2018.

[26] B. Cai and X. H. Liu, "Reliability analysis for transverse crack of concrete structure," *Applied Mechanics and Materials*, vol. 501–504, pp. 748–751, 2014.

[27] J. Li, X. Lu, J. Chen et al., "Reliability-monitoring data coupled model for concrete slab safety evaluation of CFRD and its engineering application," *Structures*, vol. 35, pp. 520–530, 2022.

[28] Y. Ji, "Fuzzy reliability analysis of nonlinear structural system based on stochastic response surface method," *Advanced Materials Research*, vol. 912–914, pp. 1268–1271, 2014.

[29] W. Chen, X. Wang, M. Liu, Y. Zhu, and S. Deng, "Probabilistic risk assessment of RCC dam considering grey-stochastic-fuzzy uncertainty," *KSCE Journal of Civil Engineering*, vol. 22, pp. 4399–4413, 2018.

[30] L. Ren, S. He, H. Yuan, and Z. Zhu, "Seismic fragility analysis of bridge system based on fuzzy failure criteria," *Advances in Civil Engineering*, vol. 2019, Article ID 3592972, 13 pages, 2019.

[31] X.-H. Xiao, P.-W. Xiao, F. Dai, H.-B. Li, X.-B. Zhang, and J.-W. Zhou, "Large deformation characteristics and reinforcement measures for a rock pillar in the houziyan underground powerhouse," *Rock Mechanics and Rock Engineering*, vol. 51, pp. 561–578, 2018.

[32] J. Li, Z. Wu, J. Chen, X. Lu, and Z. Li, "FEM-Bayesian Kriging method for deformation field estimation of earth dams with limited monitoring data," *Computers and Geotechnics*, vol. 148, Article ID 104782, 2022.

[33] Z. Wei, C. Xiaolin, Z. Chuangbing, and L. Xinghong, "Creep analysis of high concrete-faced rockfill dam," *International Journal for Numerical Methods in Biomedical Engineering*, vol. 26, no. 11, pp. 1477–1492, 2010.

[34] Q. Guo, L. Pei, Z. Zhou, J. Chen, and F. Yao, "Response surface and genetic method of deformation back analysis for high core rockfill dams," *Computers and Geotechnics*, vol. 74, pp. 132–140, 2016.

[35] J. Li, Z. Wu, and J. Chen, "An advanced Bayesian parameter estimation methodology for concrete dams combining an improved extraction technique of hydrostatic component and hybrid response surface method," *Engineering Structures*, vol. 267, Article ID 114687, 2022.

[36] Y. Jia and S. Chi, "Back-analysis of soil parameters of the Malutang II concrete face rockfill dam using parallel mutation particle swarm optimization," *Computers and Geotechnics*, vol. 65, pp. 87–96, 2015.

[37] S. Mirjalili and A. Lewis, "The whale optimization algorithm," *Advances in Engineering Software*, vol. 95, pp. 51–67, 2016.

[38] Y. Li, M. Han, and Q. Guo, "Modified whale optimization algorithm based on tent chaotic mapping and its application in structural optimization," *KSCE Journal of Civil Engineering*, vol. 24, pp. 3703–3713, 2020.

[39] H. Li, J. Deng, P. Feng, C. Pu, D. D. K. Arachchige, and Q. Cheng, "Short-term nacelle orientation forecasting using

bilinear transformation and ICEEMDAN framework," *Frontiers in Energy Research*, vol. 9, Article ID 780928, 2021.

[40] A. Hadidi, B. F. Azar, and A. Rafiee, "Efficient response surface method for high-dimensional structural reliability analysis," *Structural Safety*, vol. 68, pp. 15–27, 2017.

[41] N. Lelièvre, P. Beaurepaire, C. Mattrand, and N. Gayton, "AK-MCSi: a kriging-based method to deal with small failure probabilities and time-consuming models," *Structural Safety*, vol. 73, pp. 1–11, 2018.

[42] Y.-G. Zhao and Z.-H. Lu, *Structural Reliability: Approaches from Perspectives of Statistical Moments*, Usa, Wiley-Blackwell, Hoboken, Nj, 2021.

[43] Z. Wu, J. Li, K. Bian, and J. Chen, "Reliability analysis of slope with cross-correlated spatially variable soil properties using AFOSM," *Environmental Earth Sciences*, vol. 80, Article ID 675, 2021.